GEOSPATIAL DEEP LEARNING FOR BIOMASS AND CARBON STOCK ESTIMATION USING UAV-DERIVED CANOPY METRICS

Pimpilai WUNAPHAI [1], ***Teerawong LAOSUWAN*** [1,2*], ***Satith SANGPRADID*** [2,3*], ***Yannawut UTTARUK*** [2,4], ***Narueset PRASERTSRI*** [3], ***Thinnakon ANGKAHAD*** [1,2] ***& Piyatida AWICHIN*** [1,2]

DOI: 10.21163/GT_2026.212.08

ABSTRACT

Accurate estimation of biomass and carbon stock is important for forest monitoring and climate studies. This study developed a geospatial deep learning framework to estimate biomass and carbon stocks in rubber plantations by integrating UAV data with field measurements. The research was conducted in a rubber plantation area in northern Thailand, covering approximately 137 ha, with field data and UAV imagery collected during the 2024 growing season. UAV images were processed to generate Digital Surface Models (DSM), Digital Elevation Models (DEM), and Canopy Height Models (CHM). From these datasets, canopy structural variables such as canopy height, crown dimensions, and tree density were extracted and used as inputs for the model. Tree detection was performed using a YOLO-based deep learning approach, while field measurements were used for model training and validation. The integration of canopy structural information with deep learning improved biomass estimation at the plantation scale. The results showed strong agreement between predicted and field-measured values, with overall detection accuracy exceeding 92%. The model successfully captured spatial variation in biomass and carbon stocks across the plantation, and the estimated carbon values were consistent with plot-level observations. These findings indicate that combining UAV data, canopy structure information, and deep learning provides a practical and cost-effective approach for biomass and carbon estimation in plantation forests. The proposed workflow can also be applied to other plantation areas with similar environmental conditions.

Keywords: *Geospatial deep learning; UAV remote sensing; canopy metrics; biomass estimation; carbon stock estimation; rubber plantation*

1. INTRODUCTION

Climate change is one of the most urgent environmental issues facing the world today. Rising temperatures, shifting precipitation patterns, and more frequent extreme weather events are largely the result of increasing greenhouse gas (GHG) concentrations, especially carbon dioxide (CO_2) released from fossil-fuel combustion, land-use change, and agricultural expansion (Haidu et al., 2024; Earthobservatory, 2025; Intarat et al., 2026). These changes disrupt ecosystem processes, threaten biodiversity, and undermine long-term environmental stability (Ngthai, 2025). Strengthening natural carbon sinks has therefore become a key strategy in global climate-mitigation efforts.

[1]*Department of Physics, Faculty of Science, Mahasarakham University, Maha Sarakham, Thailand. 67010287001@msu.ac.th (PW), teerawong@msu.ac.th (TL), thinnakon.ang@gmail.com (TA), 68010262002@msu.ac.th (PA).*

[2] *Greenhouse Gas Research Center and Operations, Mahasarakham University, Maha Sarakham 44150, Thailand. satith.s@msu.ac.th (SS), yanawut.u@msu.ac.th (YU).*

[3]*Department of Geoinformatics, Faculty of Informatics, Mahasarakham University, Maha Sarakham 44150, Thailand. narueset.p@msu.ac.th (NA).*

[4]*Department of Biology, Faculty of Science, Mahasarakham University, Maha Sarakham 44150, Thailand.*

**Corresponding author: teerawong@msu.ac.th (TL) and satith.s@msu.ac.th (SS).*

Thailand has aligned its national agenda with the Paris Agreement by committing to reduce GHG emissions by 30–40% by 2030 and by setting long-term goals of achieving "Carbon Neutrality" by 2050 and "Net-Zero GHG Emissions" by 2065 (United Nations Framework Convention on Climate Change, 2025). Initiatives such as the Thailand Voluntary Emission Reduction Program (T-VER) support these goals by promoting transparent and science-based carbon-accounting practices (Thailand Greenhouse Gas Management Organization, 2025). Accurate estimation of above-ground carbon (AGC), which is typically derived from above-ground biomass (AGB) using allometric models (Laosuwan et al., 2025; Uttaruk et al., 2026), is essential for national carbon inventories, climate-policy design, and sustainable land-use planning (Plybour et al., 2025; Laosuwan, et al., 2025).

Rubber (*Hevea brasiliensis* Muell. Arg.) is a major perennial crop in Thailand, covering more than 19 million rai and serving as a major source of income for rural communities (Simon et al., 2022). Rubber plantations grow rapidly, accumulate substantial biomass, and can function as effective carbon sinks, providing both environmental and economic benefits (Blagodatsky & Cadisch, 2016; Yang et al., 2017; Tiko et a., 2025). However, estimating carbon stocks in these plantations presents several challenges (Jirakajohnkool et al., 2025; Tai et al., 2025). Traditional field-based methods that rely on measurements such as diameter at breast height (DBH) and tree height are accurate but time-consuming, labor-intensive, and costly when applied over large or remote areas (Huynh et al., 2022). These limitations have encouraged the adoption of advanced remote-sensing technologies (Angkahad et al., 2024). Unmanned aerial vehicles (UAVs) offer high-resolution imagery suitable for generating Digital Surface Models (DSM), Digital Terrain Models (DTM), and Canopy Height Models (CHM) (Angkahad et al., 2025a). These spatial products allow for detailed characterization of tree structure and canopy conditions across large areas (Angkahad et al., 2025b). UAV-based surveys reduce field workload, allow repeated monitoring, and provide spatial detail that cannot be easily achieved through ground-based measurements alone (Ecke et al., 2022; Juan-Ovejero et al., 2023).

Recent advancements in artificial intelligence (AI) have further expanded the potential of UAV-based analysis (Haidu, 2024; Intarat et al., 2024). Machine learning (ML) and deep learning (DL) models have demonstrated strong performance in tasks such as tree detection, canopy delineation, and biomass estimation in forest and agricultural systems (Aroonsri & Sangpradid, 2021; Awichin et al., 2025; Espíndola et al., 2025; Intarat et al., 2025). Object-detection frameworks like the YOLO series can identify individual tree crowns from high-resolution imagery with high accuracy, improving the reliability of tree-level assessments (Beloiu et al., 2023; Mao et al., 2025; Que et al., 2026). When integrated with canopy metrics derived from UAV photogrammetry, these models offer a powerful tool for estimating carbon stocks at scale (Zhu et al., 2022; Juan-Ovejero et al., 2023; Yan et al., 2024; Jian et al., 2025). In addition, several studies have developed geospatial deep learning frameworks that integrate UAV-derived imagery, CHM-based structural variables, and deep learning–based tree detection to estimate above-ground carbon in rubber plantations. Field measurements serve as reference data, while UAV-extracted variables support the construction of predictive models (Angkahad et al., 2025a; Mao et al., 2025; Tai et al., 2025). The goal is to produce an accurate, efficient, and reproducible approach for plantation-scale carbon assessment. The results of this study contribute to the advancement of geospatial carbon-modeling techniques and provide practical insights that support sustainable rubber-plantation management and Thailand's broader climate-mitigation objectives.

Most previous UAV-based biomass estimation studies mainly rely on statistical regression models using canopy height or vegetation indices as predictors. While these approaches provide useful estimates, they may not fully capture the structural complexity of plantation forests. In this study, we applied a different workflow by integrating UAV-derived canopy metrics with deep learning techniques for tree detection and biomass estimation. The use of a YOLO-based model allows automatic identification of individual tree crowns, which improves spatial detail compared to traditional approaches. In addition, combining field measurements with multiple canopy variables helps enhance model performance and reliability. This integrated approach provides a more flexible framework for biomass and carbon estimation in plantation environments.

2. MATERIALS AND METHODS

2.1. Study Area

The study was conducted in a rubber plantation located in Chan Chawa Subdistrict, Mae Chan District, Chiang Rai Province, covering approximately 137 ha in northern Thailand, as illustrated in **Fig. 1**. The site lies within the Mae Chan watershed at geographic coordinates near 20.236257° N and 99.972040° E. The terrain is characterized by gently undulating foothills, with elevations ranging from 410 to 480 meters above mean sea level and average slopes between 5% and 25%. The predominant soils are sandy loam to clay loam, featuring good drainage and moderate to high natural fertility, which support the long-term cultivation of perennial tree crops. The region is classified as a Tropical Monsoon Climate zone, consisting of three major seasons: summer, the rainy season, and winter. Annual mean temperatures range from 25°C to 30°C, while total annual rainfall varies between 1,700 and 1,800 millimetres. These warm and humid conditions promote vigorous rubber tree growth, resulting in substantial biomass accumulation. Such climatic and environmental characteristics make the area well suited for studies focused on above-ground biomass and carbon-stock assessment.

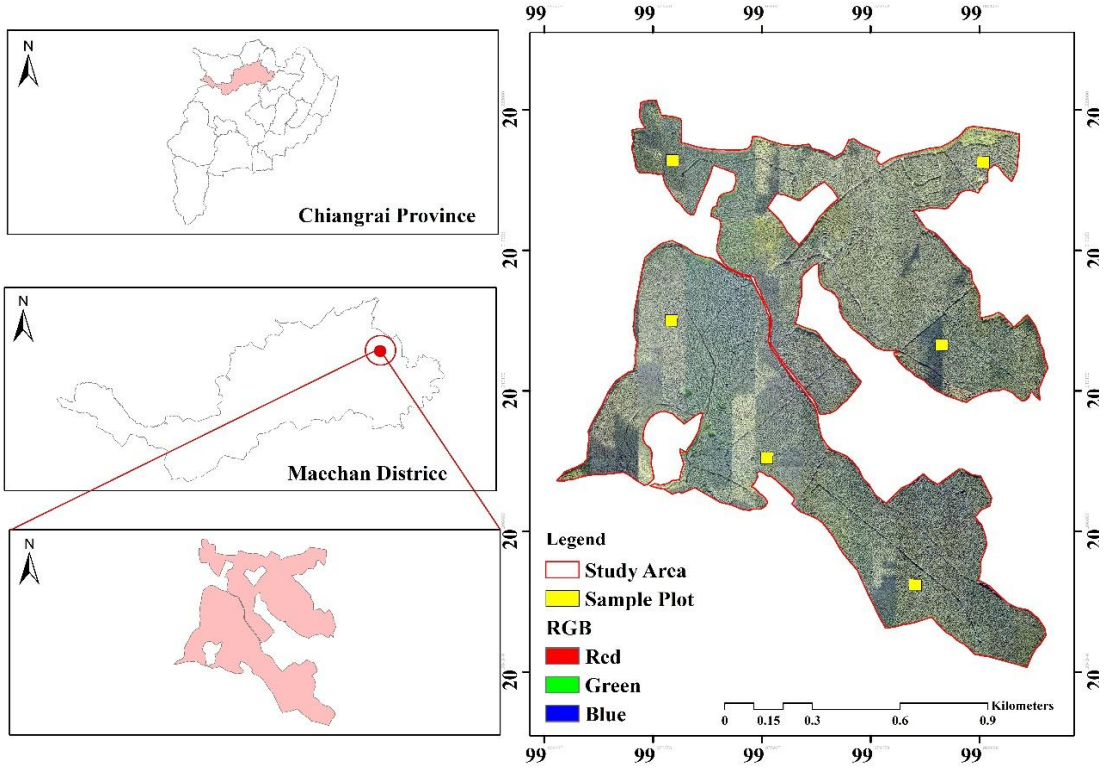

Fig. 1. Study area.

2.2. Methodology

The overall workflow of this study, illustrated in **Fig. 2**, integrates field measurements with UAV-derived datasets to support a structured approach for estimating above-ground carbon in rubber plantations. Field data collection provides core tree attributes, including DBH, height, and canopy dimensions, which are used to compute biomass and carbon through established allometric equations. These field-based estimates serve as reference data for evaluating the performance of the remote sensing and modeling components.

UAV photogrammetry represents the second major element of the workflow. High-resolution imagery is processed into point clouds, DSM, DEM, and orthophotos, from which the Canopy Height Model (CHM) is derived to capture vertical canopy structure. Machine learning and deep learning methods are then applied to identify individual trees, delineate crown features, and extract structural variables needed for biomass and carbon estimation. Model outputs are validated using regression and classification metrics to ensure accuracy and consistency, forming an integrated framework that links ground observations, spatial data, and predictive modeling. UAV photogrammetry represents the second major element of the workflow. High-resolution imagery is processed into point clouds, DSM, DEM, and orthophotos, from which the Canopy Height Model (CHM) is derived to capture vertical canopy structure. Machine learning and deep learning methods are then applied to identify individual trees, delineate crown features, and extract structural variables needed for biomass and carbon estimation. Model outputs are validated using regression and classification metrics to ensure accuracy and consistency, forming an integrated framework that links ground observations, spatial data, and predictive modeling.

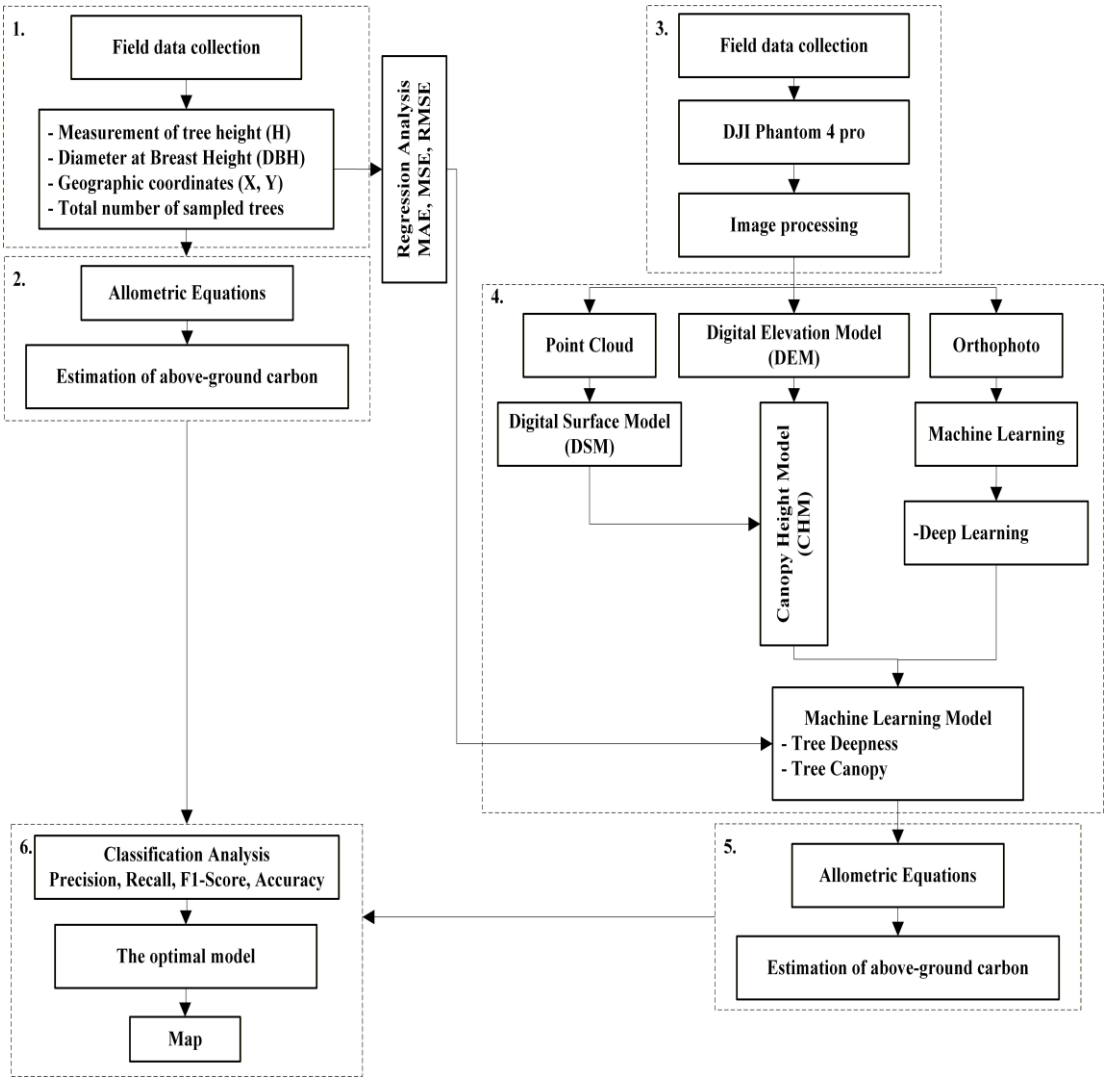

Fig. 2. Workflow of the integrated field and UAV-based deep learning methodology for above-ground carbon estimation in rubber plantations.

2.2.1. Field Survey and Data Acquisition

Field Data Collection step is represented by (1) in **Fig. 2**. Field data were collected from six 40 × 40 m sample plots established using a stratified random sampling approach to ensure representative stand conditions. Within each plot, key tree attributes were measured, including total height (H), diameter at breast height (DBH) at 1.30 m, and canopy dimensions in the north–south and east–west directions. These measurements were used to estimate above-ground biomass and served as reference data for validating the UAV-based models.

UAV Data Acquisition step is represented by (2) in **Fig. 2**. High-resolution aerial imagery was obtained using a DJI Phantom 4 Pro UAV equipped with a 20-megapixel camera and a 1-inch CMOS sensor capable of producing high-quality RGB images. The system includes an integrated GNSS module for accurate image geolocation (Angkahad et al., 2025b). Flight missions were conducted using Pix4Dcapture with a front overlap of at least 80% and a side overlap of 70% to ensure reliable image alignment. The average flight altitude ranged from 80 to 100 m above ground level. Captured imagery was processed in Agisoft PhotoScan Professional to produce essential photogrammetric outputs—including a dense point cloud, Digital Surface Model (DSM), Digital Elevation Model (DEM), and orthophoto—which served as the primary datasets for canopy-height derivation and tree-crown analysis.

2.2.2. Machine Learning–Based Data Analysis

The point cloud generated from UAV photogrammetry was used to construct two key spatial models: the Digital Elevation Model (DEM), representing the bare-earth surface without above-ground objects, and the Digital Surface Model (DSM), which includes the height of all surface features such as tree canopies and built structures. These models formed the foundational datasets for deriving canopy-height information across the study area.

The Canopy Height Model (CHM) was calculated to represent tree height above ground and served as a primary variable for estimating tree-level biomass. CHM was derived by subtracting the DEM from the DSM, where the DSM captures the maximum height of surface objects and the DEM represents the underlying terrain elevation (Angkahad et al., 2024). The CHM calculation is expressed in Equation (1) as follows:

$$CHM = DSM - DEM \tag{1}$$

where CHM is the canopy height model (m), DSM is the digital surface model (m), and DEM is the digital elevation model (m).

The selected canopy metrics were chosen because they represent key structural characteristics of plantation trees that are closely related to biomass accumulation and can be used as model inputs. Canopy height reflects tree growth and vertical structure, while crown size indicates canopy spread and overall tree volume. Tree density provides information about stand structure and competition among trees. These variables can be reliably derived from UAV-based photogrammetry and have been widely used in biomass estimation studies. Therefore, combining these canopy metrics provides meaningful input features for model development.

Deep learning techniques were applied to UAV-derived aerial imagery to analyze the structural characteristics of rubber trees and to perform automatic tree detection and counting. The YOLOv9 object-detection model was used to identify individual tree crowns from high-resolution RGB images captured by the UAV. These RGB images, composed of red, green, and blue spectral bands, served as input data for the model. The YOLOv9 framework processed each image to detect the location of rubber trees and generated bounding boxes around the identified tree crowns. The detection results were then exported into a Geographic Information System (GIS) environment to support spatial analysis. Using the Minimum Bounding Geometry (MBG) tool in ArcGIS Pro, the bounding boxes were converted into the smallest possible polygons that represent the spatial extent of each individual tree crown. This workflow enabled accurate and systematic identification and counting of rubber trees

across the plantation. The resulting tree-crown polygons also served as a key spatial layer for subsequent biomass and carbon-stock estimation (Angkahad et al., 2024). The model hyperparameters were selected based on preliminary testing and commonly recommended settings from previous studies. Parameters such as learning rate, batch size, and number of training epochs were adjusted to achieve stable training performance and avoid overfitting. The final configuration was chosen based on the best validation accuracy obtained during the training process:

$$y = \beta_1 x_1 + \beta_2 x_2 + \beta_3 x_3 + \varepsilon \tag{2}$$

where y is the estimated diameter at breast height (DBH, cm) derived from canopy structural characteristics; β_0 is the intercept; β_1, β_2, and β_3 are regression coefficients; x_1 is the canopy dimension in the north–south (NS) direction; x_2 is the canopy dimension in the east–west (EW) direction; x_3 is tree height derived from canopy structure; and ε is the error term.

Note: Calculation formulas used: $y = (29.60x_1) + (-0.88x_2) + (3.01x_3) + (-0.129.53)$

2.2.3. Above-ground Carbon Estimation in Rubber Plantations

Above-ground carbon (AGC) in the rubber plantation was estimated using the allometric equations proposed by Hytönen et al. (2018), as presented in Equations (3–6).

$$M_i = W_L + W_{LA} + W_{STUMP} \tag{3}$$

$$W_L = 0.00193 \cdot DBH^{2.499} \tag{4}$$

$$W_{LA} = 0.05155 \cdot DBH^{2.783} \tag{5}$$

$$W_{STUMP} = 0.02440 \cdot DBH^{2.470} \tag{6}$$

where DBH is the diameter at breast height measured at approximately 1.3 m above ground (cm); M_i is the total above-ground biomass of an individual tree (kg); W_L is the above-ground biomass of leaves (kg); W_{LA} is the above-ground biomass of stems and branches (kg); and W_{STUMP} is the above-ground biomass of the stump and coarse roots (kg).

$$C_{ABG} = M_i \times 0.47 \tag{7}$$

Carbon stocks were expressed in units of tCO_2. Above-ground biomass was first converted to carbon mass using a carbon fraction (CF) of 0.47, and the resulting carbon mass was then converted to CO_2 by multiplying by the molecular weight ratio of CO_2 to carbon (44/12).

2.2.4. Model Accuracy Assessment

Assessing the accuracy of the predictive model is essential to ensure that its outputs are reliable and consistent with field measurements. In this study, model accuracy was evaluated at two main levels.

The regression-based accuracy assessment quantifies how far the predicted values deviate from actual observations using standard statistical metrics. These indicators reflect both the size of prediction errors and the model's ability to explain variation in the dataset. The primary metrics used were Mean Absolute Error (MAE), Mean Squared Error (MSE), and the coefficient of determination (R^2), calculated using Equations 8–10.

$$MAE = \frac{1}{n}\sum_{i=1}^{n}\left|Actual_i - \Pr edicted_i\right| = \frac{1}{n}\sum_{i=1}^{n}\left|y_i - y_i\right| \tag{8}$$

$$MSE = \frac{1}{n}\sum_{i=1}^{n}\left(y_i - y_i\right)^2 \tag{9}$$

$$R^2 = 1 - \frac{\sum_{i=1}^{n}(y_i - y_i)^2}{\left(y_i - \overline{y}\right)^2} \tag{10}$$

where MAE is the mean absolute error; MSE is the mean squared error; R^2 is the coefficient of determination; n is the total number of samples; y_i is the observed value (field-measured AGB or carbon stock); y_i is the value predicted by the model; and $\overline{y}$ is the mean of the observed values.

2.2.5. Classification-based accuracy assessment

To evaluate the model performance in assigning rubber trees to specific diameter classes, standard classification metrics were applied. This assessment examines how well the model identifies and categorizes individual trees. The metrics used include Precision, Recall, F1-score, and overall Accuracy. Together, they offer a detailed understanding of the model's classification behavior and error patterns. These metrics were computed following Equations (11)– (14), based on established classification theory (Mohan et al., 2017).

$$\Pr ecision = \frac{TP}{TP + FP} \tag{11}$$

$$\mathrm{Re}call = \frac{TP}{TP + FN} \tag{12}$$

$$F1 - Score = 2 \times \frac{\Pr ecision \times \mathrm{Re}call}{\Pr ecision + \mathrm{Re}call} \tag{13}$$

$$Accuracy = \frac{TP + TN}{TP + TN + FP + FN} \tag{14}$$

where TP (true positive) is the number of trees correctly identified; FP (false positive) is the number of trees incorrectly identified; FN (false negative) is the number of trees that the model failed to identify; and TN (true negative) is the number of trees correctly classified as non-target cases.

3. RESULTS

3.1. Field Data Analysis Results

Field data were collected from six 40 × 40 m sample plots within the rubber plantation in Chan Chawa Subdistrict, Mae Chan District, Chiang Rai Province. Plot boundaries were established using low-error GPS at the four corners and plot center to ensure accurate spatial alignment with UAV-derived datasets. Within each plot, biometric and structural attributes of all rubber trees were recorded, including tree height (H), diameter at breast height (DBH) at 1.30 m, and canopy spread along the north–south (NS) and east–west (EW) directions. In total, 474 trees were measured. The trees had an average height of about 21 m and an average DBH of 22 cm. Mean canopy widths were 5 m (NS) and 9 m (EW), showing typical variation in crown structure found in mature rubber stands. These field measurements were used to estimate above-ground biomass (AGB) with established allometric equations. Biomass values were then converted to above-ground carbon (AGC) using a

carbon factor of 0.47. A summary of plot-level biomass and carbon estimates is presented in **Table 1**, reflecting the overall stand structure and carbon stock conditions across the sampled area.

Table 1.

Summary of Field-Based Biomass and Carbon Estimates.

Plot	Total Biomass of Rubber Trees (kg)	Above-Ground Carbon (tCO_2e)
2	21,597.19	10.15
4	31,422.85	14.77
5	32,780.05	15.41
6	30,169.42	14.18
7	28,313.47	13.31
10	29,517.43	13.87
Total	173,800.41	81.69
Average	28,966.74	13.61
Total for Entire Area	25,056,225.99	11,776.43

The field-based biomass results presented in **Table 1** show a clear and meaningful level of variation among the six sample plots. Total above-ground biomass ranged from 21,597.19 kg (Plot 2) to 32,780.05 kg (Plot 5), indicating substantial differences in stand conditions across the plantation. Plot 5 exhibited the highest biomass accumulation, exceeding the lowest plot by more than 11,000 kg. This difference reflects significant structural variability among plots, driven largely by differences in tree size distribution, canopy development, and stand density. Plot 2, which recorded the lowest biomass, likely represents areas with younger trees or reduced growth performance. Such variability aligns with known patterns of uneven growth often observed in mature rubber plantations, where microenvironmental factors and localized management practices influence stand productivity.

A similar pattern was observed in above-ground carbon (AGC) estimates, which ranged from 10.15 to 15.41 tCO_2e. Plot 5 again showed the highest carbon stock, consistent with its larger biomass, while Plot 2 had the lowest value. The difference of more than 5 tCO_2e across plots suggests a statistically meaningful spread in carbon sequestration capacity within the plantation. The mean AGC value of 13.61 tCO_2e indicates a moderate overall carbon storage potential for the study area. These results highlight that carbon variability is strongly influenced by structural heterogeneity, tree age, and site-specific growth dynamics. Collectively, the findings emphasize the importance of accounting for spatial variation in biomass and carbon assessments, particularly when scaling plot-level estimates to larger landscape units.

3.2. UAV Data Analysis Results

UAV-based carbon estimation was supported by a set of three-dimensional spatial products generated through Agisoft PhotoScan. High-resolution UAV images were processed into georeferenced outputs, including the Digital Surface Model (DSM), Digital Elevation Model (DEM), and Canopy Height Model (CHM). Together, these products provided a detailed view of terrain conditions and vegetation structure within the rubber plantation. Examples of these outputs are shown in **Fig. 3 (a-c)**. These datasets formed the foundation for extracting canopy height, detecting individual trees, and estimating carbon stocks, demonstrating the capability of UAV photogrammetry to capture fine-scale structural variation across plantation ecosystems. **Fig. 3** shows the DSM produced from UAV photogrammetry, representing the elevation of all above-ground features in the plantation. Elevation values range from about 329 to 448 meters above mean sea level. Mature, densely populated rubber stands appear in green tones, indicating higher elevations near 448 meters. In contrast, open fields, grass areas, and canopy-free zones are shown in red tones, representing elevations closer to 329 meters. This variation highlights the distribution of canopy height and reveals vertical structural differences across the landscape.

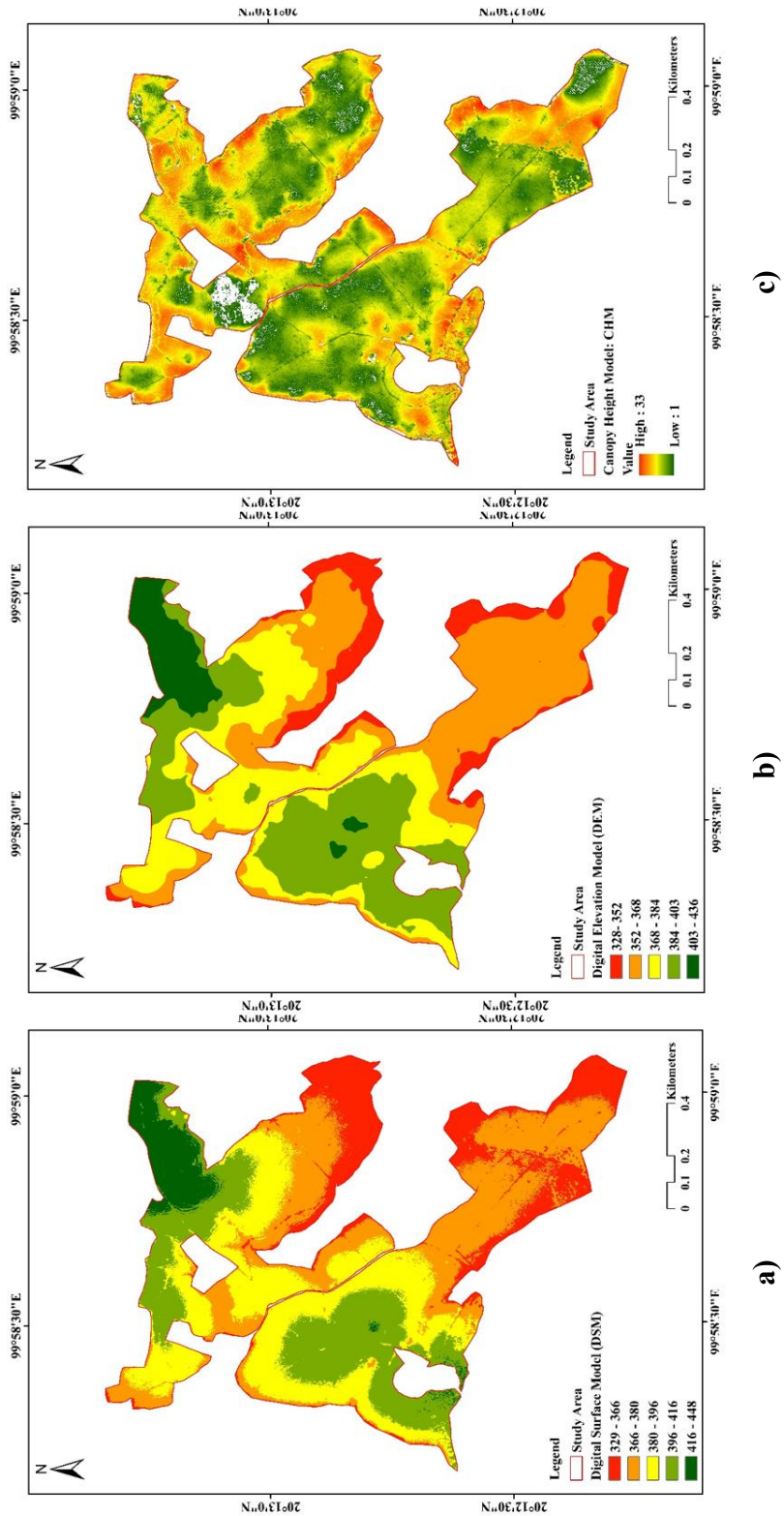

Fig. 3. (a) DSM, (b) DEM, and (c) CHM of the Rubber Plantation.

Fig. 4 presents the DEM, which reflects the bare-earth surface after removing vegetation and structures. Ground elevations range from approximately 328 to 436 meters above mean sea level. Higher terrain appears in green tones, while lower-lying areas—such as flatlands, depressions, and gently sloping surfaces—are shown in red tones. This model offers a clear visualization of underlying topographic patterns, which is essential for understanding how terrain influences tree growth and stand distribution within the plantation.

Fig. 5 displays the CHM, capturing the spatial variation in canopy height across the plantation. Canopy heights range from about 1 to 33 meters. Areas with tall, mature tree canopies are shown in red tones, indicating heights near 33 meters. Open areas or zones lacking tree cover appear in green tones, reflecting heights close to 1 meter. This model effectively represents vertical stand complexity and provides critical information for analyzing biomass patterns and overall plantation structure.

3.3. Machine Learning and Deep Learning Analysis Results

The machine learning and deep learning analyses produced strong and meaningful results in estimating above-ground carbon across the rubber plantation. The spatial products generated by the deep learning workflow offered clear insights into structural variation across the landscape. One of these outputs, the Deepness Model, highlights patterns that help explain variability in biomass and carbon accumulation. **Fig. 4** presents the Deepness Model, which divides the study area into equal-sized grid cells and classifies surface variability into five categories.

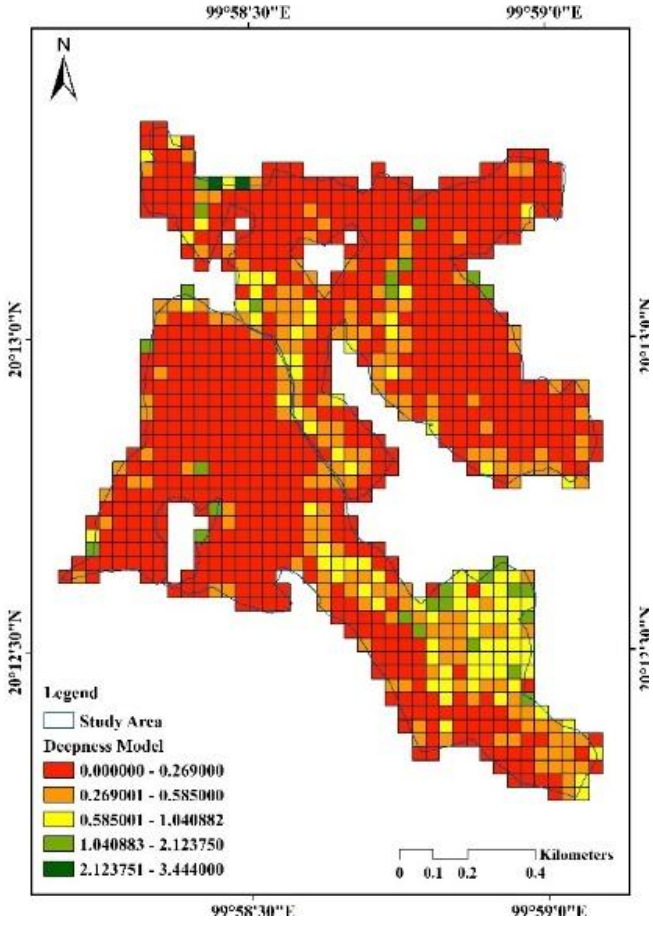

Fig. 4. Deepness Model Illustrating Surface Variability Across the Plantation.

The highest-variability areas, shown in red (2.123751–3.444000), indicate zones with pronounced elevation differences. These areas often correspond to sections of the plantation where micro-topographic shifts influence soil moisture, drainage, and canopy development. Dark orange regions (1.048083–2.123750) reflect moderately high variability, while light orange (0.585001–1.048082) represents moderate variability. Yellow areas (0.269001–0.585000) show minimal fluctuation, and the green zones (0.000000–0.269000) represent the most stable and uniform surfaces.

The spatial patterns—dominated by red and orange classes—suggest a statistically meaningful degree of micro-topographic heterogeneity across the plantation. Such variability is known to influence stand productivity, leading to measurable differences in tree growth, canopy height, and ultimately biomass accumulation. The scattered green patches mark localized stable zones with lower structural variation, serving as important reference areas for understanding baseline site conditions. Overall, the spatial classification provides key contextual information for interpreting carbon-storage patterns across the plantation.

A comparative evaluation was carried out between field-based biomass and carbon estimates and those produced by the deep learning model. Field data, including DBH and tree height, were used to compute biomass for individual tree components—leaves, stems, branches, and stumps—using standard allometric equations. These values were then converted to carbon using established conversion factors. Meanwhile, the deep learning model used UAV-derived structural data to estimate biomass and carbon through the trained predictive model. Summary values for both approaches are provided in **Table 2**, which reveals a strong level of agreement between the field-based measurements and the estimates generated by the deep learning model. Across all biomass components, the differences between the two datasets are relatively small and fall within a range that is considered acceptable for ecological and remote-sensing–based carbon assessment. For example, leaf biomass differs by about 39,000 kg, while stem and branch biomass—accounting for the largest proportion of total biomass—shows a difference of roughly 240,000 kg. Given the scale of the plantation, these deviations are minor and indicate that the model captures the overall structural patterns of the stand with high fidelity.

Total above-ground biomass values also show strong alignment: 25.06 million kg from field measurements versus 24.76 million kg from the deep learning model. The difference of only about 1.2% demonstrates the model's ability to approximate real biomass conditions with a high level of accuracy. This agreement carries over to carbon estimates as well. Field-based carbon stock totaled 11,776.43 tCO_2, while the deep learning model produced 11,639.24 tCO_2—a deviation of less than 1.2%. The carbon-to-biomass ratios follow the same trend, reflecting consistent estimation performance across methods.

A key indicator of model reliability is the average carbon density. After converting units to hectares, the field-based average is 85.06 tCO_2/ha, while the deep learning model yields 84.81 tCO_2/ha. This extremely small difference (0.25 tCO_2/ha) demonstrates statistical consistency and confirms that the model effectively represents carbon distribution at the landscape scale. Such close alignment suggests that deep learning can reliably replicate field-derived patterns of biomass and carbon accumulation, indicating strong potential for scaling carbon assessments in rubber plantations without compromising accuracy.

Table 2.

Comparison of Biomass Components and Above-Ground Carbon Estimates.

Biomass and Carbon Assessment Parameters	Field-Based Estimates	Deep Learning Estimates
Leaf biomass (kg)	320,240.12	280,990.52
Stem, branches, and above-stump biomass (kg)	21,042,496.13	21,284,651.53
Stump and root biomass (kg)	3,693,489.74	3,198,708.59
Total above-ground biomass (kg)	25,056,225.99	24,764,350.63
Carbon-to-biomass ratio ($kgCO_2e$)	11,776,426.22	11,639,244.80
Total carbon stock (tCO_2)	11,776.43	11,639.24
Average carbon density (tCO_2/ha)	85.06	84.81

3.4. Model Accuracy Assessment

The performance of the UAV-based deep learning model was evaluated using both regression-based and classification-based metrics, providing a comprehensive assessment of predictive accuracy. These complementary evaluations allowed a better understanding of how the model performs under variability in tree structure and spatial heterogeneity within the rubber plantation. Regression metrics quantified numerical differences between predicted and observed biomass and carbon values, whereas classification metrics assessed the model's ability to assign trees to the correct DBH classes. The results are summarized in **Tables 3 and 4**, and the relationship between predicted and observed biomass is illustrated in **Fig. 5**. Most data points are distributed close to the 1:1 reference line, indicating good agreement between model predictions and field measurements.

Table 3.
Error Metrics Comparing Model Predictions with Field-Measured Values.

Regression Analysis	Deep Learning
MAE	1.372
MSE	2.372
RMAE	1.165

Table 4.
Accuracy Assessment Results of the Deep Learning Model.

ID	Deep Learning
Precision	1.00
Recall	0.86
F1-score	0.925
Accuracy	92.52%

The regression metrics demonstrate statistically meaningful agreement between model outputs and field observations. The MAE of 1.372 and MSE of 2.372 indicate a narrow prediction error range, suggesting that the model is highly consistent in estimating above-ground biomass and carbon values. These errors fall well below thresholds commonly reported in plantation-based carbon modeling studies, indicating high model stability. The RMAE value of 1.165 further reinforces the model's strong predictive capability, showing limited proportional deviation relative to actual measured values. Such performance highlights the model's suitability for operational-scale biomass and carbon assessments, particularly in structurally complex plantation systems.

The classification results reveal high statistical accuracy and strong operational reliability. A Precision of 1.00 indicates zero false positives, meaning every detected tree was correctly identified. This reflects exceptional model specificity—rarely achieved in dense plantation environments where overlapping crowns can increase detection ambiguity. The Recall value of 0.86 shows that the model successfully detected the majority of trees present, with only a small fraction missed due to canopy overlap or shadowing. The F1-score of 0.925 demonstrates a well-balanced performance between Precision and Recall, confirming that the model performs robustly under varying structural conditions. The overall detection accuracy of 92.52% highlights the model's strong potential for scalable monitoring applications, particularly for carbon accounting and plantation management.

Overall, the accuracy assessment confirms that the deep learning model achieves high predictive power with statistically reliable performance across both numerical estimation and object-detection tasks. The narrow error margins, zero false positives, and high F1-score collectively indicate that the model effectively captures structural patterns that drive biomass and carbon variation in rubber plantations. These findings support its use as a scientifically robust tool for large-scale carbon stock assessment, contributing valuable data for climate reporting, ecosystem monitoring, and precision agriculture.

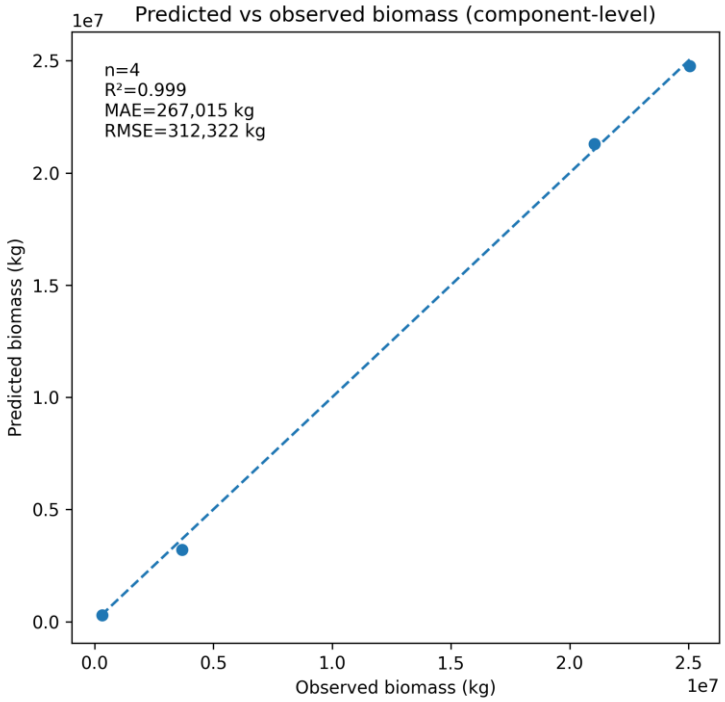

Fig. 5. Comparison between model-predicted biomass and field-measured biomass. The dashed line represents the 1:1 reference line, and evaluation metrics (R^2, MAE, and RMSE) are shown within the plot.

4. DISCUSSION

This study shows that integrating UAV photogrammetry with geospatial deep learning can improve above-ground carbon estimation in rubber plantations. Traditional field surveys often have difficulty capturing canopy structure and spatial variability over large areas. In contrast, UAV-derived datasets provide detailed information on terrain and canopy characteristics at high spatial resolution. The DSM, DEM, and CHM products clearly represented differences in canopy height and stand structure across the study plots. These variations were related to differences in tree size, canopy spread, and plantation age. The CHM was particularly useful for identifying spatial patterns of canopy height that corresponded well with observed biomass and carbon variations. Such patterns are difficult to detect using field measurements alone, especially in mature plantations.

The deep learning results further confirm the effectiveness of the proposed approach. Tree detection performance showed high precision and a strong F1-score, indicating reliable identification of individual trees. Although recall was slightly lower, this is expected in areas with dense canopy where some tree crowns overlap. Overall detection accuracy exceeded 92%, suggesting that the method performs well under typical plantation conditions.

Predicted biomass and carbon values were consistent with field measurements. The differences between predicted and observed values were relatively small, indicating that UAV-derived canopy variables can effectively represent ground conditions. This agreement is encouraging considering the uncertainties associated with both field sampling and photogrammetric processing. The results also suggest that terrain variability may influence canopy structure and carbon distribution. Areas with greater micro-topographic variation tended to show more complex canopy patterns. This indicates that terrain-related factors could be useful variables in future modeling studies.

Despite the promising results, some limitations should be considered. Detection accuracy may decrease in areas with strong canopy overlap, where individual tree crowns are partially obscured. Variations in terrain and lighting conditions may also affect the quality of UAV-derived models and influence prediction accuracy. In addition, the model was developed using data from a specific plantation environment, which may limit its direct application to other forest conditions without further calibration. Future research could improve model robustness by incorporating more diverse training data and additional environmental variables.

The results obtained in this study are comparable with those reported in previous research using UAV and machine learning approaches for biomass estimation. Several studies have shown that canopy height and crown-related variables derived from UAV data are strongly related to biomass and carbon stock. The high agreement observed between predicted and field values in this study is consistent with those findings. However, some studies reported lower prediction accuracy in areas with complex canopy structures or uneven terrain. The relatively strong performance observed here may be related to the integration of canopy metrics with deep learning‑based tree detection, which helps improve structural representation. These comparisons suggest that the proposed approach provides reliable results and contributes to the development of UAV-based biomass estimation methods.

Overall, the findings indicate that geospatial deep learning provides a practical tool for biomass and carbon estimation in rubber plantations. The approach reduces field workload, improves spatial detail, and supports repeatable monitoring at the landscape scale. This method has strong potential for plantation management, carbon accounting, and long-term environmental planning in regions with similar conditions.

5. CONCLUSION

This research demonstrates that the combination of UAV photogrammetry and geospatial deep learning is an efficient method for above-ground carbon estimation in rubber plantations. Through integration of field measurements, CHM-driven canopy metrics and YOLO-based tree detection, the workflow resulted in carbon estimates closely aligned with ground measurements. The findings further give evidence that the UAV-based information on the structure can adequately reflect between-tree variability in biomass and carbon. It decreases the demand of intensive field surveying, and still obtains high spatial resolution on plot and landscape levels. This makes the approach practical for repeated monitoring within plantation environments where time, cost or access limits field data collection. The analysis also underscores the importance of including terrain-related information as the Deepness Model indicates that micro-topographic variation affects canopy structure and carbon distribution. To validate the method, it is suggested that future work trialling the proposed approach be conducted on a range of plantations with variable age, management and environment. Inclusion of other data sources, such as high-resolution multispectral UAV imagery, LiDAR or satellite time series data could be expected to increase the robustness of models assembled for mapping in this area. Together, this study illustrates the feasibility of geospatial deep learning as an application to biomass and carbon mapping in plantation forestry and associated landcape contexts.

ACKNOWLEDGMENTS

This research project was financially supported by Mahasarakham University.

REFERENCES

Angkahad, T., Chokkuea, W., Sangpradid, S., Uttaruk, Y., Viriyasatr, K., & Laosuwan, T. (2025a). The assessment of above-ground biomass and carbon sequestration in community forests using UAV technology. *Defence Technology Academy Journal, 7*(15), R11–R28.

Angkahad, T., Laosuwan, T., Sangpradid, S., Prasertsri, N., Uttaruk, Y., Phoophathong, T., & Nuchthapho, J. (2024). An empirical analysis of above-ground biomass and carbon sequestration utilizing UAV photogrammetry and machine learning techniques. *IEEE Access, 12*, 186740–186752. https://doi.org/10.1109/ACCESS.2024.3514074

Angkahad, T., Laosuwan, T., Sangpradid, S., Prasertsri, N., Uttaruk, Y., Phoophathong, T., & Nuchthapho, J. (2025b). Developing a drone-based machine learning for spatial modeling and analysis of biomass and carbon sequestration in forest ecosystems. *Engineered Science, 35*, 1508. https://doi.org/10.30919/es1508

Awichin, P., Laosuwan, T., Sangpradid, S., Uttarak, Y., Phoophathong, T., Leammanee, S., & Nuchthapho, J. (2025). UAV multispectral indices and linear regression for estimating biomass and carbon in rubber plantations. *IEEE Access*, 13, 215845–215860. https://doi.org/10.1109/ACCESS.2025.3644408

Aroonsri, I. & Sangpradid, S. (2021). Artificial Neural Networks for the classification of shrimp farm from satellite imagery. *Geographia Technica*, 16(2), 149–159. https://doi.org/10.21163/GT_2021.162.12

Blagodatsky, S., Xu, J., & Cadisch, G. (2016). Carbon balance of rubber (*Hevea brasiliensis*) plantations: A review of uncertainties at plot, landscape and production level. *Agriculture, Ecosystems & Environment, 221*, 8–19. https://doi.org/10.1016/j.agee.2016.01.025

Earthobservatory. (2025). *The carbon cycle.* https://earthobservatory.nasa.gov/features/CarbonCycle

Ecke, S., Dempewolf, J., Frey, J., Schwaller, A., Endres, E., Klemmt, H.-J., Tiede, D., & Seifert, T. (2022). UAV-based forest health monitoring: A systematic review. *Remote Sensing, 14*(13), 3205. https://doi.org/10.3390/rs14133205

Espíndola, R. P., Picanço, M. M., de Andrade, L. P., & Ebecken, N. F. F. (2025). Applications of machine learning methods in sustainable forest management. *Climate, 13*(8), 159. https://doi.org/10.3390/cli13080159

Haidu, I. (2024). Geography's future is technical: A letter from the editor. *Geographia Technica*, 19(2), i–vi. https://doi.org/10.21163/GT_2024.192.23

Haidu, I., Ionac, N., & Irașoc, A. (2024). The new climatic normals and their impact on bioclimatic indices: Case study: Oradea (Romania). *Present Environment and Sustainable Development*, 18(2), Article 2001. https://doi.org/10.47743/pesd2024182001

Huynh, T., Lewis, T., Applegate, G., Pachas, A. N. A., & Lee, D. J. (2022). Allometric equations to estimate aboveground biomass in spotted gum (*Corymbia citriodora* subspecies variegata) plantations in Queensland. *Forests, 13*(3), 486. https://doi.org/10.3390/f13030486

Hytönen, J., Kaakkurivaara, N., Kaakkurivaara, T., & Nurmi, J. (2018). Biomass equations for rubber tree (*Hevea brasiliensis*) components in southern Thailand. *Journal of Tropical Forest Science, 30*(4), 588–596. https://doi.org/10.26525/jtfs2018.30.4.588596

Intarat, K., Kuankhamnuan, P., & Jangsawang, W. (2026). Flood mapping in Phra Nakhon Si Ayutthaya, Thailand, utilizing Sentinel-1 SAR imagery and deep learning approaches. *Geographia Technica, 21*, 1–18. https://doi.org/10.21163/GT_2026.211.04

Intarat, K., Netsawang, P., Narawatthana, S., Promaoh, C., & Chuenkamol, S. (2025). Integrating spectral and texture indices with machine learning for rice leaf area index estimation in Suphan Buri, Thailand. *Geographia Technica, 20*(1), 207–227. https://doi.org/10.21163/GT_2025.201.15

Intarat, K., Nuengjumnong, N., Sae-Jung, J., Jangsawang, W., Yoomee, P., & Panboonyuen, T. (2024). Deep residual neural networks with self-attention for landslide susceptibility mapping. In *GIS-IDEAS 2024* (pp. 1–6). IEEE. https://doi.org/10.1109/GIS-IDEAS63212.2024.10990879

Jian, K., Lu, D., & Li, G. (2025). Modeling forest carbon stock based on sample plots and UAV LiDAR data and examining its vertical characteristics in Wuyishan National Park. *Remote Sensing, 17*(3), 377. https://doi.org/10.3390/rs17030377

Jirakajohnkool, S., Wongsai, S., Sanpayao, M., & Wongsai, N. (2025). Age-based biomass carbon estimation and soil carbon assessment in rubber plantations. *Forests, 16*(11), 1652. https://doi.org/10.3390/f16111652

Juan-Ovejero, R., Elghouat, A., Navarro, C. J., Reyes-Martín, M. P., Jiménez, M. N., Navarro, F. B., & Castro, J. (2023). Estimation of aboveground biomass and carbon stocks of *Quercus ilex* saplings using UAV RGB imagery. *Annals of Forest Science, 80*, 44. https://doi.org/10.1186/s13595-023-01210-x

Laosuwan, T., Uttaruk, Y., Nakapan, S., Itsarawisut, J., & Plybour, C. (2025). Evaluation of tree biomass and carbon sequestration through remote sensing and field methods. *Geographia Technica*, 33–43. https://doi.org/10.21163/gt_2025.201.04

Laosuwan, T., Uttaruk, Y., Sangpradid, S., Butthep, C., & Leammanee, S. (2023). The carbon sequestration potential of silky oak (*Grevillea robusta*). *Forests, 14*(9), 1824. https://doi.org/10.3390/f14091824

Mao, Z., Abdi, O., Uusitalo, J., Laamanen, V., & Kivinen, V.-P. (2025). Super-resolution supporting individual tree detection using aerial imagery. *ISPRS Journal of Photogrammetry and Remote Sensing, 224*, 251–271. https://doi.org/10.1016/j.isprsjprs.2025.04.005

Mohan, M., Silva, C. A., Klauberg, C., Jat, P., Catts, G., Cardil, A., Hudak, A. T., & Dia, M. (2017). Individual tree detection from UAV-derived canopy height models. *Forests, 8*(9), 340. https://doi.org/10.3390/f8090340

Ngthai. (2025). *What is the carbon cycle?* https://ngthai.com/science/31560/carbon-cycle/

Plybour, C., Laosuwan, T., Uttaruk, Y., Awichin, P., Rotjanakusol, T., Itsarawisut, J., & Singharath, M. (2025). An investigation of plant species diversity, above-ground biomass, and carbon stock. *Diversity, 17*(6), 428. https://doi.org/10.3390/d17060428

Que, H., Gao, H., Shan, W., Liu, M., An, J., Deng, F., Feng, S., Yang, X., & Mu, L. (2026). FM-SAM: Tree crown delineation using SAM and YOLOv10. *Computers and Electronics in Agriculture, 240*, 111162. https://doi.org/10.1016/j.compag.2025.111162

Tai, H., Rao, C., Li, X., Li, H., & Li, C. (2025). Extracting rubber tree parameters and estimating carbon storage using airborne LiDAR. *PLOS ONE, 20*(8), e0330768. https://doi.org/10.1371/journal.pone.0330768

Thailand Greenhouse Gas Management Organization. (2025). *What is T-VER?* https://ghgreduction.tgo.or.th/en/what-is-t-ver/what-is-t-ver.html

Tiko, J. M., Ndjadi, S. S., Obandza-Ayessa, J. L., Mweru, J. P. M., Michel, B., Beeckman, H., Rakotondrasoa, O. L., & Hulu, J. P. M. T. (2025). Carbon sequestration potential in rubber plantations. *Earth, 6*(2), 21. https://doi.org/10.3390/earth6020021

Uttaruk, Y., Laosuwan, T., Sangpradid, S., Samek, J. H., Butthep, C., Rotjanakusol, T., Dumrongsukit, S., & Rouylarp, Y. (2026). Species-Specific Allometric Models for Biomass and Carbon Stock Estimation in Silver Oak (*Grevillea robusta*) Plantation Forests in Thailand: A Pilot-Scale Destructive Study. *Forests*, *17*(1), 100. https://doi.org/10.3390/f17010100

Yan, Y., Lei, J., & Huang, Y. (2024). Forest aboveground biomass estimation using UAV-LiDAR and machine learning. *Sensors, 24*(21), 7071. https://doi.org/10.3390/s24217071

Yang, X., Blagodatsky, S., Liu, F., Beckschäfer, P., Xu, J., & Cadisch, G. (2017). Rubber tree allometry and carbon stocks in subtropical China. *Forest Ecology and Management, 404*, 84–99. https://doi.org/10.1016/j.foreco.2017.08.013

Zhu, X., Chen, B., Wang, C., & He, H. (2022). Above-ground biomass estimation using UAV LiDAR and allometric models. *Remote Sensing, 14*(5), 1024. https://doi.org/10.3390/rs14051024